SANDIA REPORT
SAND2021-14653
Printed November 2021

Sandia National Laboratories

A Medium Frequency RF Sensor for Detection of Magnetized Quark Nuggets

John J. Borchardt

Prepared by
Sandia National Laboratories
Albuquerque, New Mexico
87185 and Livermore,
California 94550

Issued by Sandia National Laboratories, operated for the United States Department of Energy by National Technology & Engineering Solutions of Sandia, LLC.

Available to DOE and DOE contractors from
U.S. Department of Energy
Office of Scientific and Technical Information
P.O. Box 62
Oak Ridge, TN 37831

Telephone: (865) 576-8401
Facsimile: (865) 576-5728
E-Mail: reports@osti.gov
Online ordering: http://www.osti.gov/scitech

Available to the public from
U.S. Department of Commerce
National Technical Information Service
5301 Shawnee Rd
Alexandria, VA 22312

Telephone: (800) 553-6847
Facsimile: (703) 605-6900
E-Mail: orders@ntis.gov
Online order: https://classic.ntis.gov/help/order-methods/

ABSTRACT

It is hypothesized that dark matter is composed of particles called quark nuggets, and further that these particles have a permanent magnetic dipole moment. If this hypothesis is true, calculations predict that a magnetized quark nugget (MQN) will oscillate when encountering the Earth's magnetosphere, and emit RF radiation between 30kHz and 30MHz. To support testing this hypothesis, a loop antenna sensor was designed and developed, which is described in this report. This sensor operates between 300kHz and 3MHz and achieves about -11dBfT/√Hz sensitivity at 1.5MHz.

ACKNOWLEDGEMENTS

Marquan Chaney contributed to the modeling and design of the coil geometries described in this report.

CONTENTS

1. Introduction 8
   1.1. Galactic Noise 8
2. Loop Antenna Design 10
3. Amplifier 13
4. Testing 17

LIST OF FIGURES

Figure 1. Top: Galactic noise temperature; middle: galactic noise brightness; bottom: galactic noise equivalent Tesla per root Hertz. 9
Figure 2. FEMM calculations of a 12-turn coil; left: "transmit" sim with 1A in coil gives the inductance; right: "receive" sim with 1T impressed gives the transfer function. 11
Figure 3. Four-arm frame and 3D printed hub onto which wire turns are strung to form a square-spiral loop antenna. 12
Figure 4. ISL55210TQFN-EVAL1Z schematic, from the user's manual. 13
Figure 5. QUCS model of the coil and amplifier. 14
Figure 6. QUCS model output. Left: input-output signal; right: input-output noise. 14
Figure 7. Left: Comparison of galactic noise and amplifier noise at the amplifier input; 15
Figure 8. Measured 50 Ohm s-parameters of the modified SL55210TQFN- EVAL1Z. 16
Figure 9. 5-turn coil (set against a block of polystyrene foam) and amplifier in an anechoic chamber; a commercial loop antenna is visible at left for injecting a test signal into the sensor. . 17
Figure 10. Instrument display; left: noise measurement (KKOB 770 as well as some other AM broadcast stations are visible despite the shielding provided by the anechoic chamber); 18

LIST OF TABLES

Table 1. Measured sensor noise data 18
Table 2. Measured sensor signal data 18

This page left blank

ACRONYMS AND DEFINITIONS

Abbreviation	Definition
MQN	Magnetized Quark Nugget
SNR	Signal to Noise Ratio
RTI	Referred to Input
LNA	Low Noise Amplifier
FDA	Fully Differential Amplifier
SRF	Self-Resonant Frequency

1. INTRODUCTION

It is hypothesized that dark matter is composed of particles called quark nuggets, and further that these particles have a permanent magnetic dipole moment [1]. If this hypothesis is true, calculations predict that a magnetized quark nugget (MQN) will oscillate when encountering the Earth's magnetosphere, and emit RF radiation between 30kHz and 30MHz [2]. To support experimental testing of this hypothesis, a loop antenna sensor operating between 300kHz and 3MHz was designed and developed. It is envisioned that this sensor might ultimately orbit the Earth and thus be exposed to galactic noise while the Earth's ionosphere would substantially shield the sensor from atmospheric lightning discharge noise as well as terrestrial broadcast signals. Two other loop antennas (30-300kHz and 3-30MHz) were designed using computer modeling but were not constructed or tested. General information on the design and development of the type of sensors described in this report is available in [3] and [4].

1.1. Galactic Noise

One design goal is to have thermal noise generated by the sensor itself to be less than that due to received galactic noise (noise emanating from the core of the Milky Way galaxy) at the sensor output. When this condition is achieved, the signal-to-noise ratio (SNR) of a hypothesized radiating MQN is maximized. However, this is a challenge because galactic noise is relatively small; this is a somewhat surprising result since galactic noise is characterized by a noise temperature of millions of Kelvin, whereas COTS low noise amplifiers (LNAs) have noise temperatures on the order of 300K.

The apparent contradiction is explained when we calculate the received voltage due to the galactic noise field and compare it with the input referred noise voltage of a typical room temperature LNA. We can do this by first converting the galactic noise spectral brightness into units of magnetic field. The brightness (units W/sr/m^2/Hz—this can be understood as Watts per Hz per steradian of source per meter squared of receiver, OR Watts per Hz per meter squared of source per steradian of receiver) is given by the Rayleigh-Jeans law:

$$B_\nu(T) = \frac{2\upsilon^2 k_B T}{c^2}$$

where k_B is the Boltzmann's constant, T is the temperature in Kelvin and c is the speed of light. The noise temperatures (taken from [2]) are shown in Fig. 1, along with the corresponding spectral brightness. Assuming an isotropic receiver viewing angle of 4π steradians, we may convert the spectral brightness into a spectral power flux density S (with units W/ Hz/m^2) and, then, using the impedance and permeability of free space, into an equivalent magnetic flux density B (T/√Hz). This is done in Fig. 1 which shows that the galactic noise field strength is on the order of 1e-17 T/√Hz.

Now, a typical input-referred noise voltage for any kind of low-noise amplifier, whether audio, RF or microwave, is about 1nV/√Hz. Thus, to transform the galactic noise field to this level requires a loop antenna with a transfer function of 10^8 V/T. It turns out that this is quite a large transfer function with respect to practical considerations. In a loop antenna, additional Volts per Tesla may be achieved by increasing the number turns, however, with additional turns comes additional capacitance. This capacitance forms a resonator with

the loop inductance and determines a self-resonant frequency (SRF). Near this frequency, the loop antenna will not respond predictably to an incident changing magnetic flux density and the loop impedance properties (which in turn impact the noise properties of the LNA) are uncontrolled; thus, the SRF limits the number of turns that may be used. We therefore seek a loop antenna design with as high a transfer function as possible, but with a self-resonance somewhat above the highest frequency we wish to use it at (preferably at least a factor of two).

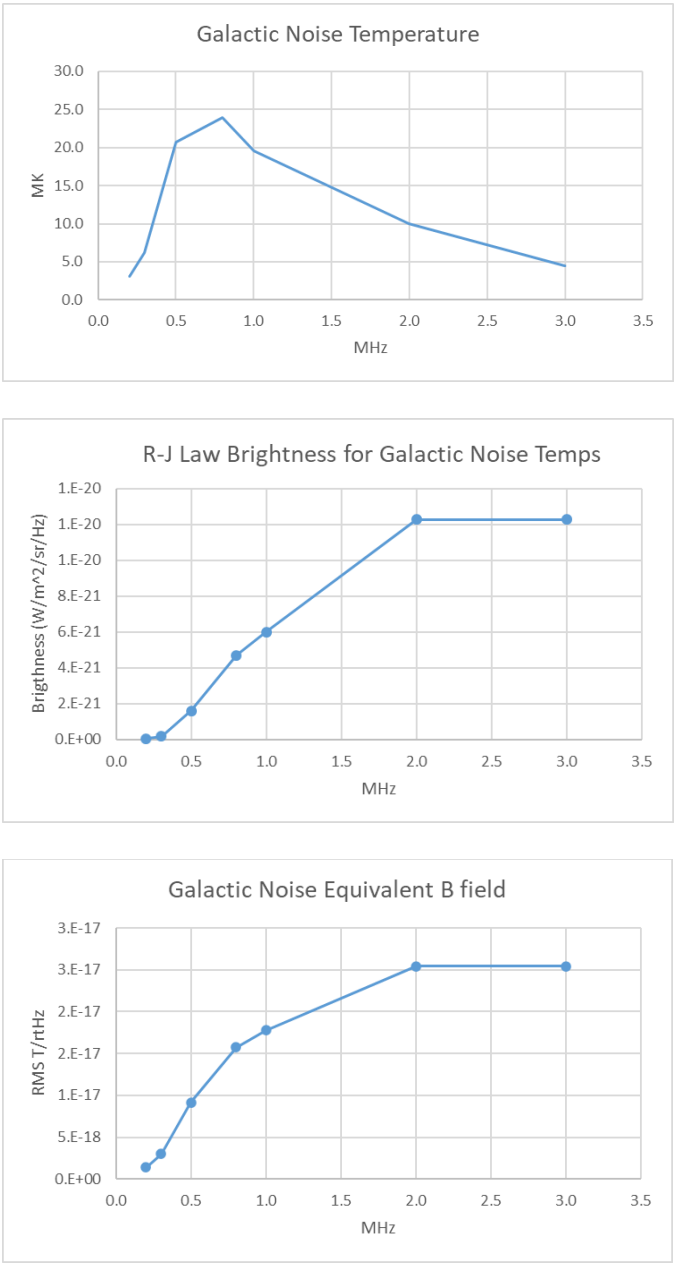

Figure 1. Top: Galactic noise temperature; middle: galactic noise brightness; bottom: galactic noise equivalent Tesla per root Hertz.

2. LOOP ANTENNA DESIGN

As in prior work, FEMM [5], a freely-available software tool, was used to design receiver coils. In FEMM, a coil is approximated as isolated axi-symmetric turns; interconnections between the turns are made analytically. A Lua script was used to generate coil geometries, run the time-harmonic magnetic calculations, and output the geometry inductance and transfer function. In addition, the Lua script was extended to drive the FEMM electrostatic solver and calculate the Maxwell capacitance matrix [6]. Here, 1V is applied to each conductor one at a time and the resulting charge on the remaining conductors is calculated. The resulting capacitance data is written as a SPICE netlist and read into QUCS [7], a freely-available circuit solver. In QUCS, the nodes associated with the first and last turns are driven with a 1 Ampere AC source and the resulting voltage is used to solve for an equivalent capacitance. This capacitance is then combined with the FEMM-solved inductance to yield an estimate of the self-resonant frequency.

Initial studies showed that flat spiral geometries seem to have better performance (i.e., more Volts per Tesla for a given SRF) than long solenoid-type geometries. The use of a high-permeability (i.e., ferrite) core was avoided due to increased size/weight and the potential for nonlinearity, temperature dependence and RF loss; besides, the effective permeability of any low-aspect ratio ferrite body that would "fit" with a flat-spiral coil is severely limited by large demagnetizing factors. An initial candidate design for the 300k-3MHz band was developed; some simulation results are shown in Fig. 2. The design is 12 spiral turns of 36 AWG wire spaced at 2" with 54" (1.37 meter) overall diameter. This design has about 32 meters of wire total (about $\lambda/10$ at 3MHz); the total area is about 8 square meters. The 1MHz-calculated inductance and open-circuit transfer function are 130μH and 51.6MV/T, respectively (the transfer function is, to first order, proportional to frequency). The calculated effective capacitance is 5.0pF, yielding an 6MHz self-resonant frequency. The corresponding coil reactance, which has implications for the sensor frequency response and amplifier noise performance, is 816Ω at 1MHz.

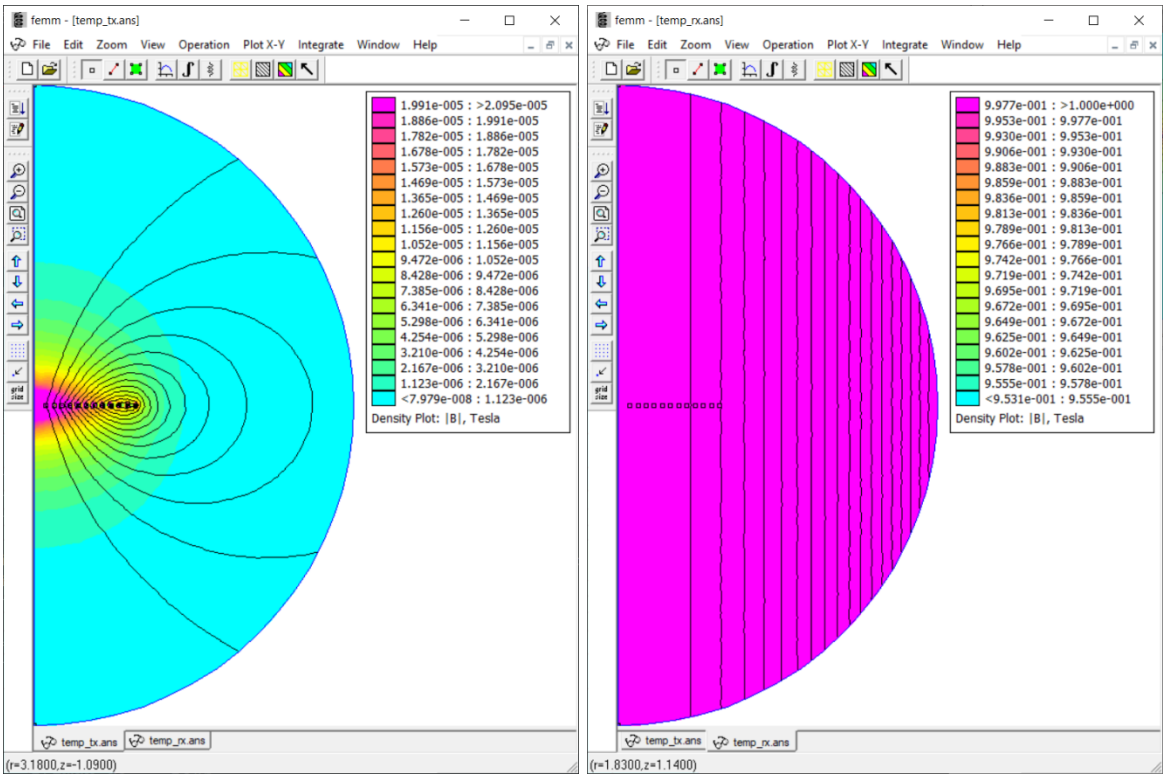

Figure 2. FEMM calculations of a 12-turn coil; left: "transmit" sim with 1A in coil gives the inductance; right: "receive" sim with 1T impressed gives the transfer function.

The coil was constructed slightly differently than modeled. A four-arm frame with a 3D printed hub was assembled as shown in Fig. 3. The arms are G10 tubes with 1" outer diameter. A series of angled slits was cut in each tube at 2" spacing; between these slits, wire is strung, forming a square-spiral coil. The axi-symmetric modeling results given above can be easily adjusted to account for this square implementation; inductance, transfer function and capacitance should be multiplied by $4/\pi$.

An immediate practical problem was encountered in that 36AWG wire is too fragile for the relatively large length scales and open geometry of the coil. Fortunately, simulation (and some experiment) shows the wire diameter impacts the coil properties only slightly; 18 AWG wire was used instead. The 12-turn loop described above was thus constructed; its inductance was about 160µH (as measured on an LCR meter) but the self-resonant frequency (as measured on a vector network analyzer) was found to be about 1MHz—far lower than that calculated—making this design unusable for the 300kHz-3MHz band.

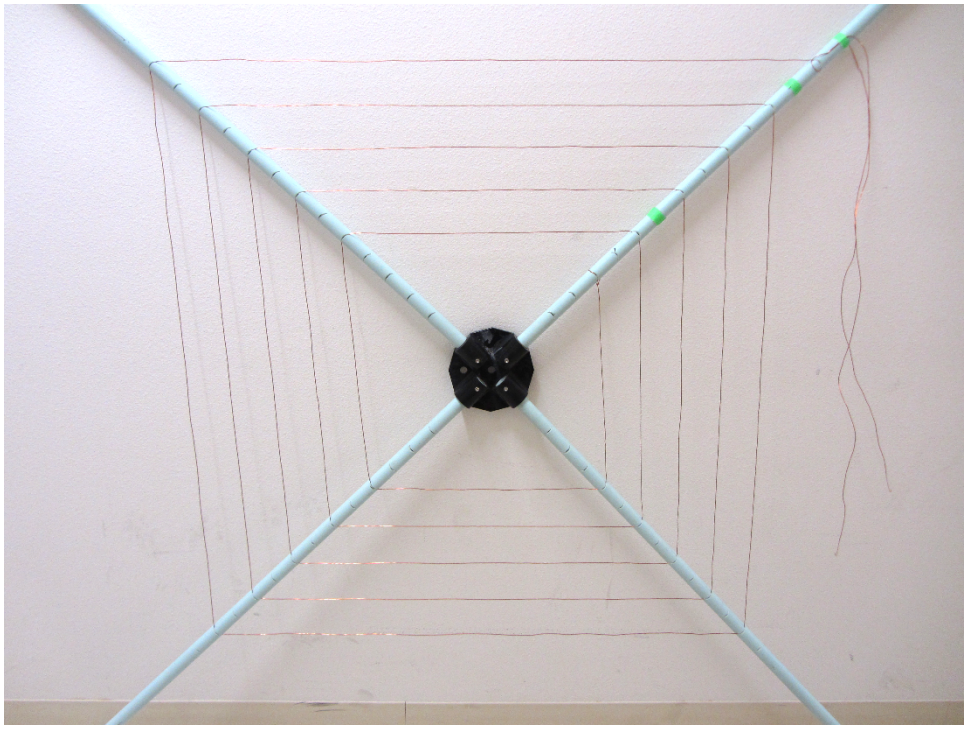

Figure 3. Four-arm frame and 3D printed hub onto which wire turns are strung to form a square-spiral loop antenna.

The antenna was adjusted empirically to 5 turns of 18AWG wire spaced at 4" with the inner turn starting at a radius of 10". The diagonal span of the outermost turn is about 60" (1.52 meters). The measured inductance was 36μH and measured SRF was 4.5MHz. Modeling of this geometry, adjusted by the $4/\pi$ factor, yields a predicted inductance of 43μH and open-circuit transfer function of 29MV/T.

3. AMPLIFIER

Fully differential amplifiers (FDAs) have been used to good effect in similar applications in the past [3]. FDAs provide low noise, low distortion, high gain, inherent common-mode rejection and easy adjustability of both input impedance and gain. Because this is a broad-band application (the sensor is desired to operate over a decade), no capacitive matching network is used between the coil and the amplifier. For simplicity of calibration and to make best use of the limited analog-to-digital converter dynamic range, the "self-integrating" regime [3] is sought wherein the coil reactance is much larger than the amplifier input impedance. This results in a flat (versus frequency) signal output despite the fact that the induced coil open-circuit voltage is proportional to frequency.

The Intersil ISL55210 fully differential amplifier was selected for this application. This is a relatively unique device that offers 0.85nV/√Hz and 5pA/√Hz noise and 4GHz of gain-bandwidth product with about 35mA of current consumption from a single 3.3V supply. The SL55210TQFN-EVAL1Z evaluation board was procured. With reference to the evaluation board user manual schematic shown in Fig. 4, several changes were made: 1) feedback resistors R5 and R8 were changed to 5.0k Ohms, 2) input resistors R3 and R4 were changed to 10.2 Ohms, 3) R13 and R14 were removed from the output chain. Changing the feedback and input resistors sets the FDA gain at approximately 5.0k/10.2 ~ 500V/V = 54dB. Changing the input resistors causes the loop to operate in the "self-integrating" regime (the reactance of 36µH at 300kHz is 68 Ohms, larger than the R3+R4 = 20.4 Ohms of total input resistance). Finally, removing the output resistors reduces the output attenuation (thereby increasing overall gain) at the expense of source match.

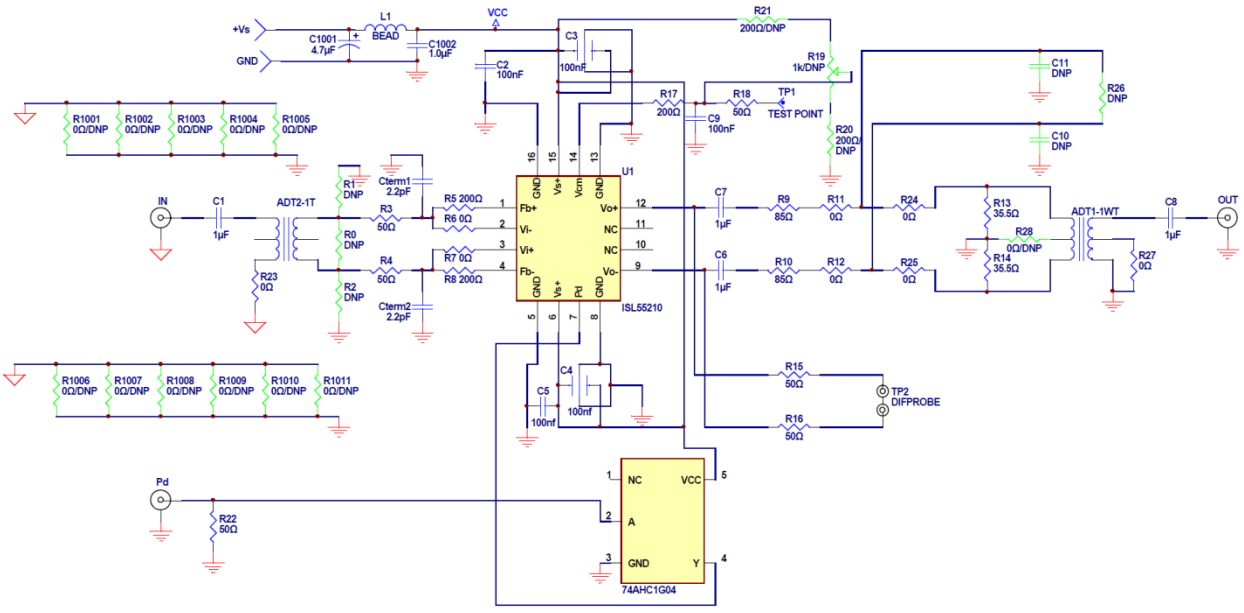

Figure 4. ISL55210TQFN-EVAL1Z schematic, from the user's manual.

A QUCS [7] model of the coil and amplifier is shown in Fig. 5. V1, I1 and I2 are noise sources. The capacitor C1 represents the amplifier input capacitance, however, within the feedback bandwidth of the amplifier, it does not impact the coil self-resonance. The QUCS op-amp models are ideal, with no bandwidth limitation. The turns ratio of the input and output transformers are 1:1.4 and 1:1 (as they are on the evaluation board); here, they are modeled as ideal (with no loss).

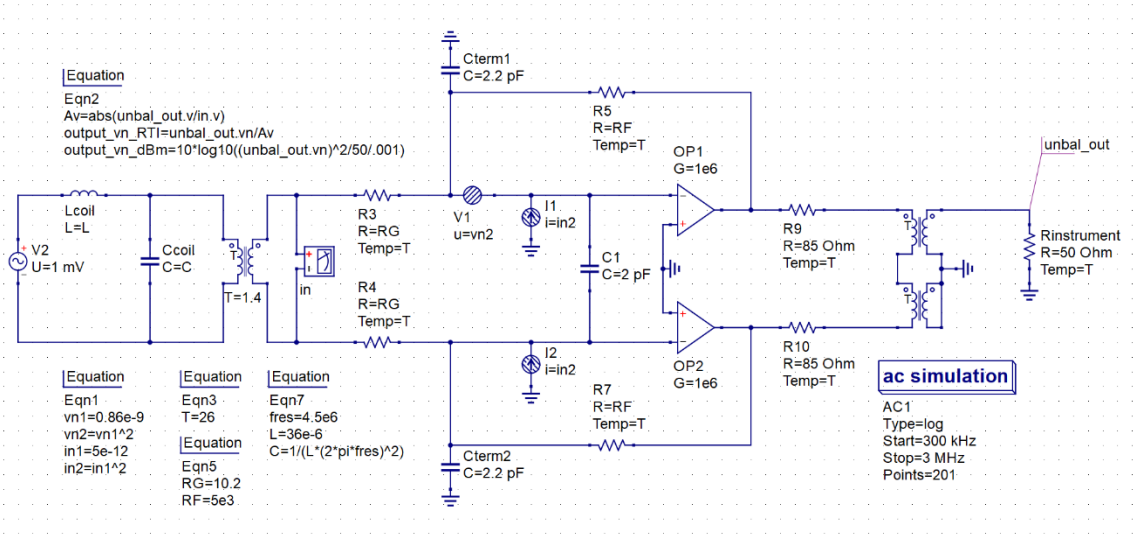

Figure 5. QUCS model of the coil and amplifier.

QUCS model results are shown in Fig. 6. Here, the input and output signal decrease with frequency because the source amplitude is a constant 1mV; with the actual antenna, the input voltage will be proportional to frequency (in accord with Faraday's law of induction), thereby producing a flat frequency response.

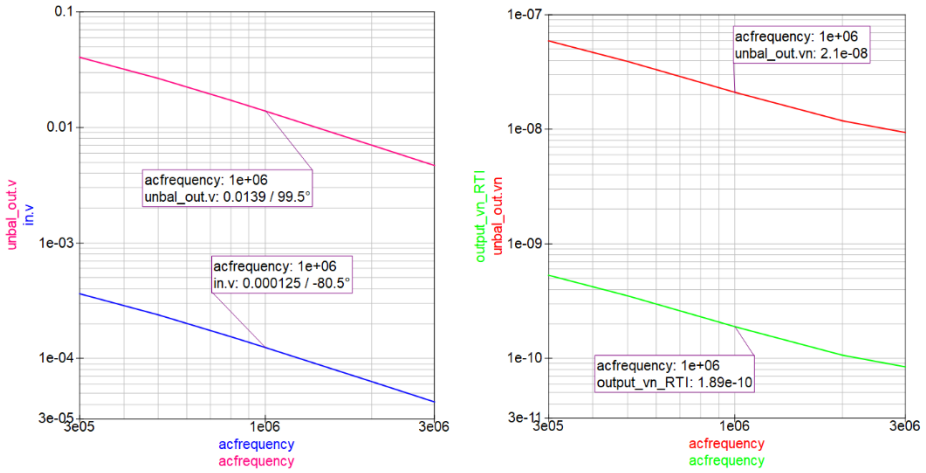

Figure 6. QUCS model output. Left: input-output signal; right: input-output noise.

Interestingly, Fig. 6 shows the input-referred noise voltage drop from the expected ~1nV/√Hz at 300kHz to ~0.2nV/√Hz at 1MHz. This is a beneficial byproduct of the large coil reactance (which increases with frequency): at frequencies above the L-R time-constant formed by the coil and the FDA input resistors, the noise gain is reduced, whereas the signal gain remains constant, set by the ratio of the input and feedback resistors.

From Fig. 6, we see that the 1mV (open-circuit) signal in the model is reduced at the input to the FDA; this is due to the voltage-divider formed by the coil reactance and FDA input resistors. Considering the input transformer turns ratio $T = 1.4$, the voltage division factor is:

$$T\frac{2R_{in}}{(2R_{in} + j\omega L_{coil})},$$

which, for R_{in}= 10.2Ω and L_{coil} = 36µH, is about 0.123 at 1MHz (and such is seen in Fig. 6.) From Fig. 6, we see that the overall gain of the amplifier circuit, including input and output voltage divider effects, is about 111V/V; in the actual amplifier, this gain will be reduced a few dB according to the loss of the input and output transformers.

Accounting for input and output voltage divider effect, Fig. 7 compares the analytically calculated galactic noise and QUCS-calculated amplifier noise referred to the amplifier input. We see the that the amplifier approaches the galactic noise only at the high end of the band; at the low end of the band, the amplifier noise dominates. We note that if the input voltage division factor were smaller, the effective Volts per Tesla of the sensor (and the galactic noise at the amplifier input) would be higher. Ignoring for a moment that the amplifier noise performance depends on its input loading, this could potentially increase the sensitivity, however doing so while remaining in the self-integrating (flat-frequency response) regime is a challenge given the empirically encountered limits on coil SRF. The parameters selected represent a working compromise among all competing effects; the predicted sensitivity, also shown in Fig. 7, ranges from about -11dBfT/√Hz at 300kHz to -27dBfT/√Hz at 3MHz.

The 50 Ohm s-parameters of the SL55210TQFN-EVAL1Z, with the modifications described above, are shown in Fig. 8. About 35dB of gain (in 50 Ohms) is available to 30MHz. The input match to 50 Ohms is poor due to the 10.2Ω input resistors, however, in this application the antenna is not 50 Ohms, and this configuration provides the desired performance properties in terms of noise and flat signal response, as described above.

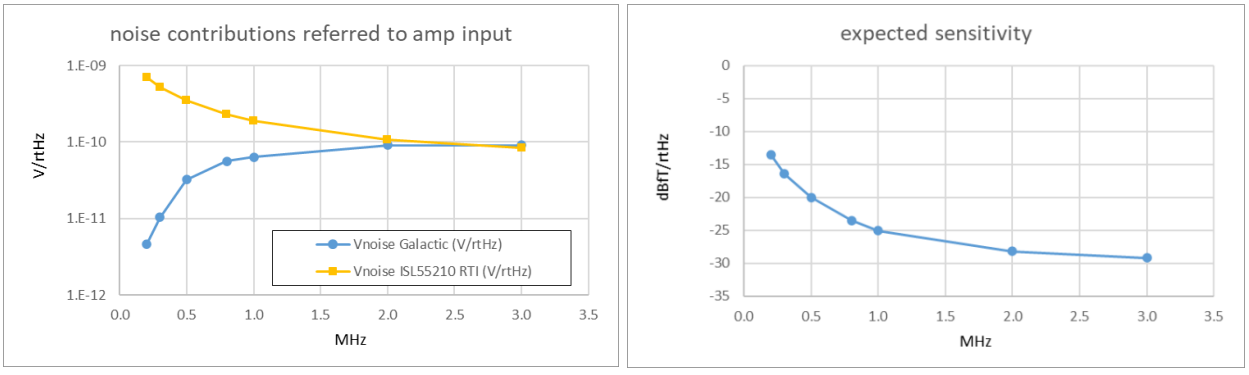

Figure 7. Left: Comparison of galactic noise and amplifier noise at the amplifier input; right: predicted sensor sensitivity.

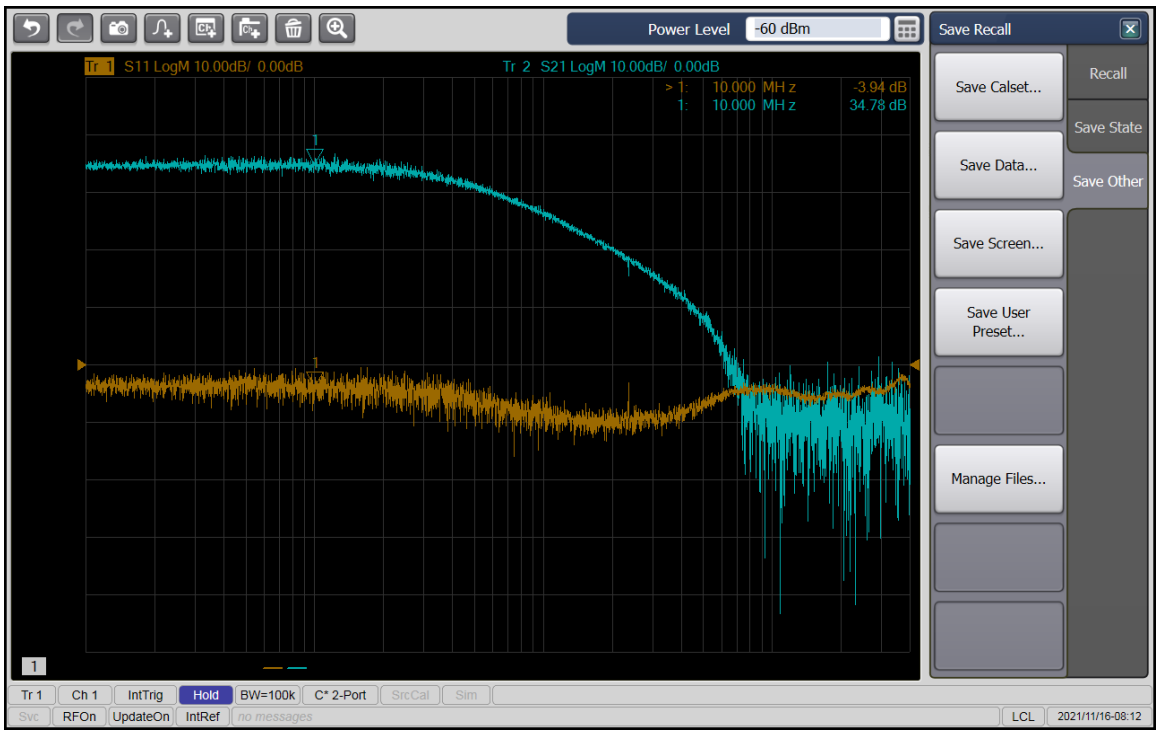

Figure 8. Measured 50 Ohm s-parameters of the modified SL55210TQFN-EVAL1Z.

4. TESTING

The 5-turn coil was connected to the modified ISL55210TQFN-EVAL1Z evaluation board and set up in the anechoic chamber in Sandia National Laboratories building 891 as shown in Fig. 9; the chamber provides only very limited anechoic properties in the band of interest, however, it provides significant shielding against external signals (such as AM broadcast signals) so that the isolated noise performance of the system can be measured. A 12" diameter single-turn loop antenna, AH Systems SAS-564, was located about 1.73 meters from the plane of the coil to provide a test signal to the coil.

To provide amplifier bias, A DC power supply was located outside of the chamber and connected via a BNC cable; the FDA power supply rejection ratio will reduce the coupling of any stray signals (e.g., AM broadcast) to the amplifier output. An Agilent 89441A vector signal analyzer is used as a characterization receiver; it, too, is located outside the chamber and connected to the amplifier via BNC cable because the instrument display generates radio noise in the band of interest. This instrument has been used for these kinds of measurements in the past [3] because it has two unbalanced inputs that can be used together as a single balanced input, however, because the output of the ISL55210TQFN-EVAL1Z evaluation board is unbalanced, any standard spectrum analyzer could have been used.

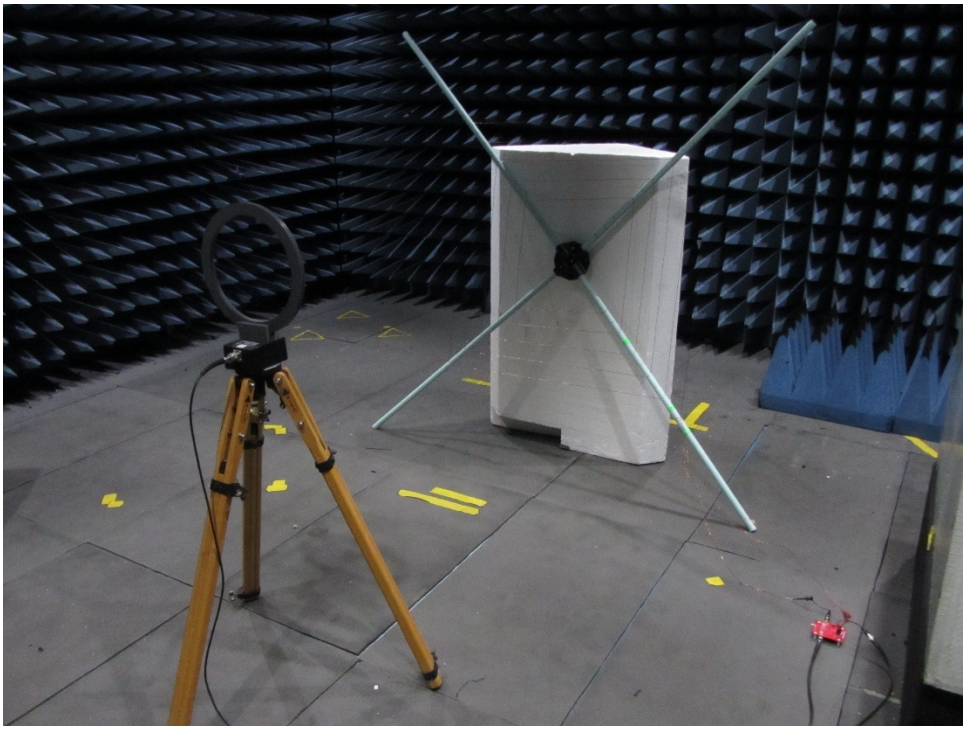

Figure 9. 5-turn coil (set against a block of polystyrene foam) and amplifier in an anechoic chamber; a commercial loop antenna is visible at left for injecting a test signal into the sensor.

Broadband noise data shown in Table I was measured; it shows that the sensor noise output dominates the instrument thermal noise and that the noise floor decreases about 7dB when the 5-turn coil is connected in place of a 50 Ohm termination input (the circuit modeling described above predicts a 9dB decrease). With a 100Hz resolution bandwidth, -116dBm noise is measured near band center with the coil connected to the amplifier, as seen in Fig. 10. This corresponds to 35.4nV RMS/√Hz—somewhat higher than the 21nV RMS/√Hz seen in the modeling results of Fig. 6.

Table 4. Measured sensor noise data

Amplifier input	Amplifier bias	100Hz RBW noise measured
50Ω termination	0VDC	-123 dBm
50Ω termination	3.3VDC/32mA	-109 dBm
5-turn coil	3.3VDC/32mA	-116 dBm

A 1.5MHz signal at -30dBm is injected into the SAS-564 loop antenna; analytical calculations show that the loop current should be about 0.39mA and that the resulting on-axis field at the 5-turn coil is about 1.1pT. FEMM modeling of the loop and coil geometry yields about 0.8pT field across the face of the 5-turn coil; we use this field strength in the following. Fig. 10 shows the resulting signal out of the sensor is -69.8dBm in 50 Ohms, implying a sensor transfer function of 113MV/T. Together, the ratio of the noise voltage to transfer function implies a sensitivity of 0.271fT/√Hz, or -11dBfT/√Hz. This is somewhat short of the expected sensitivity shown in Fig. 7; however, it is still excellent performance. Sensitivity will decrease as the noise floor rises at the low end of the band; this is also predicted by modeling results of Fig. 6. Table 2 shows that the signal output of the sensor is substantially flat with frequency for a -30dBm constant amplitude stimulus; due to the large amplitude of the signal, the noise floor in this plot does not reflect the true system noise floor.

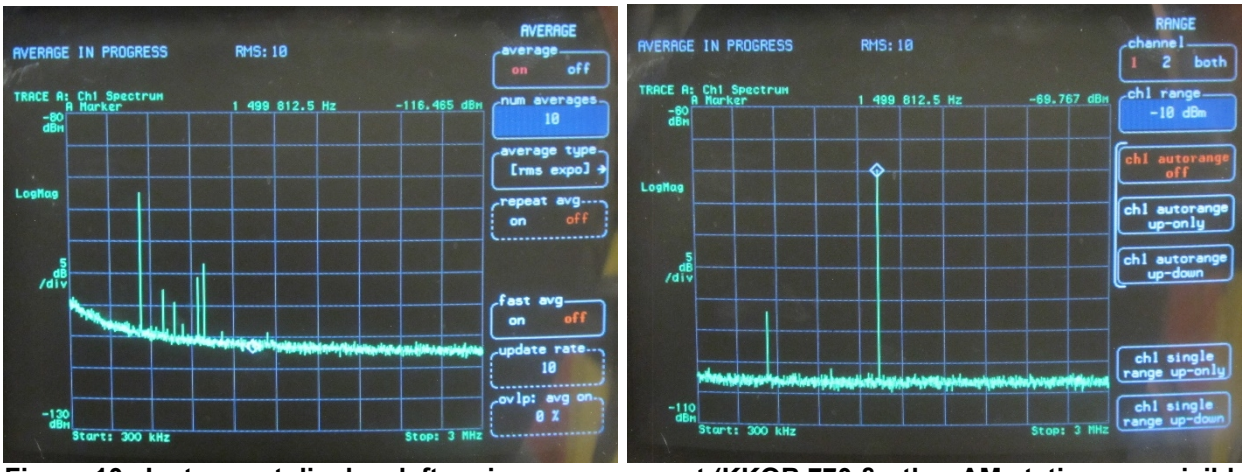

Figure 10. Instrument display; left: noise measurement (KKOB 770 & other AM stations are visible despite the shielding provided by the anechoic chamber); right: signal measurement at 1.5MHz.

Table 2. Measured sensor signal data

Frequency (MHz)	Sensor output (dBm)
0.3	-69.4
0.5	-69.4
0.8	-69.4
1.0	-69.5
2.0	-70.0
3.0	-70.5

REFERENCES

[1] VanDevender, J.P., Shoemaker, I.M., Sloan, T. et al. "Mass distribution of magnetized quark-nugget dark matter and comparison with requirements and observations," Sci Rep 10, 17903, 2020.

[2] VanDevender, J.P., Buchenauer, C.J., Cai, C. et al. "Radio frequency emissions from dark-matter-candidate magnetized quark nuggets interacting with matter," Sci Rep 10, 13756, 2020.

[3] John Borchardt, "Low Frequency Magnetic Field Sensors" Sandia National Laboratories report SAND2019-5915 (OUO/ECI ITAR), 2019.

[4] John Borchardt, "Low Frequency Magnetic Field Sensor Analytics" Sandia National Laboratories report SAND2021-2684 (Unclassified Unlimited Release), 2021.

[5] Finite Element Method Magnetics (FEMM) software. Available online: https://femm.info

[6] "The Maxwell Capacitance Matrix," FastFieldSolvers, SRL white paper. Available online: https://www.fastfieldsolvers.com/Papers/The_Maxwell_Capacitance_Matrix_WP110301_R02.pdf

[7] Quite Universal Circuit Simulator (QUCS) software. Available online: http://qucs.sourceforge.net/

DISTRIBUTION

Email—Internal

Name	Org.	Sandia Email Address
John Borchardt	5363	jjborch@sandia.gov
Technical Library	01977	sanddocs@sandia.gov

Email—External [redacted]

Name	Company Email Address	Company Name
Pace VanDevender	pacevan@gmail.com	VanDevender Enterprises, LLC

Sandia National Laboratories

Sandia National Laboratories is a multimission laboratory managed and operated by National Technology & Engineering Solutions of Sandia LLC, a wholly owned subsidiary of Honeywell International Inc. for the U.S. Department of Energy's National Nuclear Security Administration under contract DE-NA0003525.